JOURNAL OF MATERIALS SCIENCE 32 (1997) 6183–6189

Modelling pressure-assisted densification by power-law creep

S. BHATTACHARYA, K. JAKUS, I. GROSSE
Department of Mechanical and Industrial Engineering, University of Amherst, MA 01003, USA

Densification of ceramic powders by power-law creep during pressure-assisted compaction is analysed. The proposed densification model is based on two existing power-law creep densification models: one for a relative density up to 0.9 (stage I) and the other for densities above 0.9 (stage II). Using these two models independently in their respective density ranges for predicting hot pressing of homogeneous alumina powder results in a discontinuity in the densification rate time history curves as well as in the radial and hoop stress time histories in the compact. To eliminate these discontinuities a novel method of combining the two models into a single unified model is presented. Blending of the models is based on the assumption that porosity changes gradually from being completely open at the beginning of compaction to completely closed at full density. Experimental data generated by hot pressing homogeneous alumina cylindrical compacts at two different temperatures of 1400 and 1450 °C at different pressures were used to obtain the material creep constants that were employed in the unified model.

Nomenclature

A_1	creep constant for stage I ($MPa^{-n_1} s^{-1}$)
A_2	creep constant for stage II ($MPa^{-n_2} s^{-1}$)
D	relative density of powder
D_0	initial relative density of powder (at start of compaction)
$(\dot{E}_{ij})_i$	creep strain rate tensor components (i = I, II corresponding to stages I and II, respectively) (s^{-1})
n_1, n_2	creep exponents for stage I and stage II models, respectively
p	hydrostatic stress equal to $-\frac{1}{3}(\sigma_{11} + \sigma_{22} + \sigma_{33})$ (MPa)
q	von Mises stress equal to $\{\frac{1}{2}(\sigma_{11} - \sigma_{22})^2 + (\sigma_{22} - \sigma_{33})^2 + (\sigma_{33} - \sigma_{11})^2 + 6(\sigma_{12}^2 + \sigma_{23}^2 + \sigma_{31}^2)]\}^{1/2}$ (MPa)
δ_{ij}	Kronecker delta
σ_{ij}	Cauchy stress tensor (MPa)

1. Introduction

Pressure-assisted densification currently is a common technology for the manufacture of powder metallurgy and ceramic components. Therefore, it is important to predict densification behaviour and the residual stress generation in parts fabricated by pressure-assisted densification. In particular, with the advent of composites and functionally gradient materials, one needs to be able to predict densification and stress behaviour in systems with gradients in properties such as initial density and composition.

Two recent models for predicting pressure-assisted densification have been developed by Kuhn and McMeeking [1] and by Sofronis and McMeeking [2]. These models are based on power-law creep that is believed to be the predominant densification process in hot pressing and hot isostatic pressing (HIP) of ceramic materials. The first model by Kuhn and McMeeking [1] applies to low relative densities ($D < 0.9$). This density region is typically referred to as stage I. The second model by Sofronis and McMeeking [2] was developed for the higher-relative-density region ($D > 0.9$), known as stage II.

Predictions by the above models [1, 2] have been compared with experimental data by several investigators. In the case of HIP homogeneous compacts the stage I model reduces to an earlier model proposed by Ashby [3] which was used to predict the densification of low-carbon steel and alumina powders. The predictions used independently determined creep constants from the literature for the respective powders. Good agreement between the data and the predictions was reported. The stage I model was also used to predict uniaxial compression of alumina powders [1]. The predictions were compared with data obtained using pre-sintered specimens that were pressed under different pressures. The model's constants were adjusted such that the predicted axial strain rate matched the data at a relative density of 0.8. The model was then used to predict strain rates at different densities in the range $0.65 < D < 0.9$. Good agreement was obtained between the predictions and the data. A model similar to the stage II model [2] was used to predict the final part shape of hot isostatically pressed nickel-based

0022–2461

superalloy (Astroloy) powders [4]. The part shape predictions were based on creep constants from uniaxial creep compression and HIP densification tests. The predicted final shape of the parts compared well with the experiments. Liu *et al.* [5] also used the stage II model to predict densification by HIP, hot pressing and uniaxial compression of a porous intermetallic alloy (Ti–14 wt% Al–21 wt% Nb). The creep constants for these predictions were obtained from compression creep tests of the fully dense alloy. These predictions also fit the experimental data well. It should be noted that the above-discussed predictions were compared with data at either low or high relative densities (stage I or stage II). None of these predictions spanned the entire densification range from the initial low density to the final high density.

In order to predict the densification history from initial low density at the beginning of compaction to the final, almost full density at the end of compaction, a method is needed to bridge the two existing densification models. This need is especially important in those cases where significant density gradients develop in the compact. In such cases, creep and densification calculations have to be made simultaneously for both low and high densities. Such a situation was considered by Song *et al.* [6] for hot pressing homogeneous copper powder where density gradients developed owing to die wall friction. These researchers blended the stage I and stage II models in a narrow overlapping region of relative densities. By this approach, they predicted relatively smooth transition of density from stage I to stage II. However, the evolution of stresses during compaction was not considered. As will be shown, the prediction of a smooth transition in density does not guarantee a smooth evolution in the state of stress. This is especially true in cases where substantial deviatoric stresses exist during densification. To make the predictions free of such discontinuities, a new method of blending is proposed.

2. The densification models

The existing power-law creep models considered in this paper [1, 2] have been developed on the assumption that creep is the dominant mechanism for densification. The difference between the two models results from the assumed powder morphology differences in the two stages. In stage I the porosity is considered to be open and interconnected with discrete necks bridging adjacent particles. Densification is assumed to occur by the growth and creep deformation of the necks. In contrast, pores in stage II are considered to be closed (hollow spheres) and isolated from each other. Densification in this case occurs by the shrinkage of these pores due to the creeping of the surrounding material. These morphological perspectives lead to different densification processes that are represented mathematically in terms of creep strain rate tensors.

The components of the creep strain rate tensor, $(E_{ij})_{\mathrm{I}}$, developed by Kuhn and McMeeking [1] for stage I are given by (see Nomenclature for definitions)

$$(\dot{E}_{ij})_{\mathrm{I}} = (\dot{\varepsilon})_{\mathrm{I}}\left(a_{\mathrm{I}}\frac{3}{2}\frac{\sigma_{ij}+p\delta_{ij}}{q}-\frac{1}{3}b_{\mathrm{I}}I_{ij}\right) \quad (1)$$

where

$$(\dot{\varepsilon})_{\mathrm{I}} = \frac{2}{3}C_{\mathrm{cr}}\left[|p|^{(n_1+1)/n_1}+\left(\frac{2q}{3}\right)^{(n_1+1)/n_1}\right]^{n_1-1} \times\left[\frac{1}{2}|p|^{2/n_1}+\left(\frac{2q}{3}\right)^{2/n_1}\right]^{1/2} \quad (2)$$

$$C_{\mathrm{cr}} = A_1\frac{27\pi}{16\times 3^{1/2}}\frac{(1-D_0)^{n_1-0.5}(D-D_0)^{0.5}}{[3D^2(D-D_0)]^{n_1}} \quad (3)$$

$$a_{\mathrm{I}} = \frac{(2q/3)^{1/n_1}}{[\frac{1}{2}|p|^{2/n_1}+(2q/3)^{2/n_1}]^{1/2}} \quad (4)$$

$$b_{\mathrm{I}} = \frac{\frac{3}{2}|p|^{1/n_1}\,\mathrm{sign}(p)}{[\frac{1}{2}|p|^{2/n_1}+(2q/3)^{1/2}]^{1/2}} \quad (5)$$

For stage II, Sofronis and McMeeking [2] have derived a creep strain rate tensor, whose components $\dot{E}_{ij}$ are given by

$$(\dot{E}_{ij})_{\mathrm{II}} = (\dot{\varepsilon})_{\mathrm{II}}[a_{\mathrm{II}}\tfrac{3}{2}(\sigma_{ij}+p\delta_{ij})-\tfrac{1}{3}b_{\mathrm{II}}pI_{ij}] \quad (6)$$

where

$$(\dot{\varepsilon})_{\mathrm{II}} = A_2(a_{\mathrm{II}}q^2+b_{\mathrm{II}}p^2)^{(n_2-1)/2} \quad (7)$$

$$a_{\mathrm{II}} = \left(\frac{2-D}{D}\right)^{2n_2/(n_2+1)} \quad (8)$$

$$b_{\mathrm{II}} = \left(\frac{n_2(1-D)}{[1-(1-D)^{1/n_2}]^{n_2}}\right)^{2/(n_2+1)}\left(\frac{3}{2n_2}\right)^2 \quad (9)$$

The constants A_1, A_2, n_1 and n_2 are the power-law creep constants for stage I and stage II, respectively. It should be noted that A_1 and A_2 can be temperature dependent; therefore,

$$A_1 = A_1^*\exp\left(-\frac{Q_1}{RT}\right) \quad (10)$$

$$A_2 = A_2^*\exp\left(-\frac{Q_2}{RT}\right) \quad (11)$$

where Q_1 and Q_2 are the apparent activation energies for stage I and stage II respectively.

The trace of the above strain rate tensors given by Equations 1 and 6 result in the following differential equation for densification rates:

$$\frac{\dot{D}}{D} = -(\dot{E}_{kk})_{\mathrm{I}} = -(\dot{\varepsilon})_{\mathrm{I}}b_{\mathrm{I}} \quad \text{for stage I} \quad (12)$$

$$\frac{\dot{D}}{D} = -(\dot{E}_{kk})_{\mathrm{II}} = -(\dot{\varepsilon})_{\mathrm{II}}pb_{\mathrm{II}} \quad \text{for stage II} \quad (13)$$

3. Implementation of the models into a finite-element code

To predict densification and stress history during pressure-assisted compaction of complex geometric shapes, finite-element analysis (FEA) has to be used. Therefore, the two densification models (Equations 1 and 6) were implemented into a FEA code ABAQUS

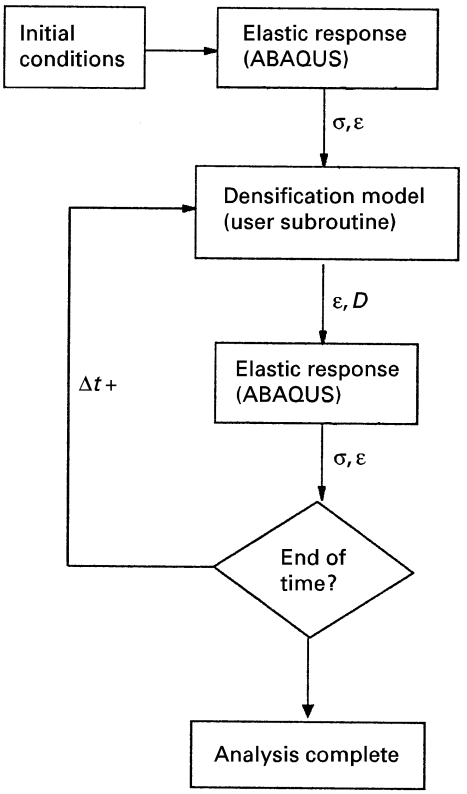

Figure 1 Schematic diagram of solution scheme.

(registered trademark of Hibbitt Karlsson and Sorensen Inc., Pawtucket, RI, USA) with a user-defined CREEP subroutine. Accordingly, the stress tensor is calculated by ABAQUS whereas, the creep and densification strain are calculated within user-defined subroutine. The flow chart for the computation is shown in Fig. 1. The sequence of calculations is as follows. First, the initial elastic stress distribution within the powder compact is calculated for the applied load using ABAQUS. Next the stage I densification model is called to calculate the incremental creep deformation and densification strain and to update the relative density. The newly calculated values are returned to ABAQUS which recalculates the stress tensor. This sequence is repeated for subsequent time steps until the end of stage I. At this time the user-defined routine is changed to stage II, and the calculation sequence is continued until the end of the densification period.

ABAQUS has a flexible routine to calculate the deformation and density changes based on user-supplied equations [7]. This routine was developed to provide a generic methodology to calculate the deformation and swelling (increase in density) of soils. The routine is based on the following equation for the strain increment in a given time step:

$$\Delta E_{ij} = \Delta\varepsilon^{cr}\frac{3}{2}\frac{\sigma_{ij}+p\delta_{ij}}{q}+\tfrac{1}{3}\Delta\varepsilon^{sw}I_{ij} \qquad (14)$$

where $\Delta\varepsilon^{cr}$ represents the creep deformation strain increment and $\Delta\varepsilon^{sw}$ represents the swelling strain increment. The functional dependences of $\Delta\varepsilon^{cr}$ and $\Delta\varepsilon^{sw}$ on stress must be provided by the user. Although the routine was developed to account for swelling (increase in density), it is also applicable for the decrease in density. Therefore, this ABAQUS routine provides a convenient way to implement the densification models (Equations 1 and 6). In particular it should be noted that the functional form of Equation 14 is the same as Equations 1 and 6 except that the strain rate in Equation 14 is given in a discretized incremental form. By comparing the first and second terms on the right-hand side of Equations 1 and 6 with those of Equation 14, one obtains the following strain increments:

$$(\Delta\varepsilon^{sw})_I = -(\dot{\varepsilon})_I b_I \Delta t \qquad (15)$$

$$(\Delta\varepsilon^{cr})_I = (\dot{\varepsilon})_I a_I \Delta t \qquad (16)$$

$$(\Delta\varepsilon^{sw})_{II} = -(\dot{\varepsilon})_{II} p b_{II} \Delta t \qquad (17)$$

$$(\Delta\varepsilon^{cr})_{II} = (\dot{\varepsilon})_{II} a_{II} q \Delta t \qquad (18)$$

Furthermore, the density increment is calculated as follows:

$$D^{new} = D + \dot{D}\Delta t \qquad (19)$$

where $\dot{D}$ is given by Equations 12 and 13.

When the user-defined subroutine is called by ABAQUS, instantaneous values of the stress and the relative density are passed into the subroutine, which then calculates the incremental strains and the new relative density by Equations (14)–(19). The variation in elastic modulus and Poisson's ratio with density was derived by solving the equations for the density-dependent bulk and shear moduli of powders [8]. Finally, the subroutine returns the newly calculated values to ABAQUS. This process is repeated for each Gauss (integration) point for each element of the finite-element mesh at every time step.

4. Prediction of hot pressing of alumina powders

To illustrate the effect of transition from one model to the other, the prediction of hot pressing of alumina powder compacts was performed in a rigid cylindrical die with a rigid single-action punch. Four-node linear axisymmetric elements were used to represent the powder in the axisymmetric die. The punch and the die walls were considered to be rigid surfaces. The contact between the powder and the punch and that between the powder and the die walls were assumed to be frictionless. Because of the symmetry of the problem, only the top half of the cylindrical compact was modeled. A schematic diagram of the finite-element model is shown in Fig. 2.

The constants for the models were obtained by fitting the predictions to experimental data. Data were obtained for alumina powder that was hot pressed in a cylindrical die of 25 mm diameter with pressures of 5, 10 and 20 MPa at 1400 °C and pressures of 5, 7 and 12 MPa at 1450 °C [9]. A density versus time curve was obtained for each applied pressure. The results of the 12 MPa at 1450 °C test was used to obtain a preliminary estimate for the creep constants A_1, A_2, n_1 and n_2. The low-density portion (relative density below 0.9) of these data was used to obtain the constants

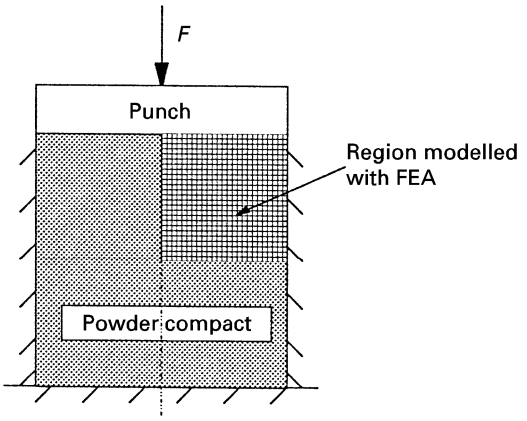

Figure 2 Schematic diagram of finite-element model.

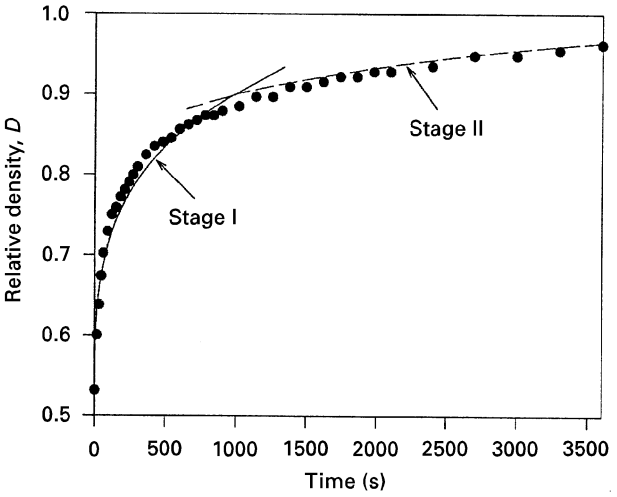

Figure 3 Discontinuity between the stage I (—) and stage II (– –) models (alumina powders hot pressed at 12 MPa and 1450 °C). (●), experiment.

n_1 and A_1 of the stage I model (Equations 1–5), and the high-density portion (relative density above 0.9) was used for the constants n_2 and A_2 of the stage II model (Equations 6–9).

The fit of the stage I and the stage II models to the data for an applied pressure of 12 MPa at 1450 °C is shown in Fig. 3. It is seen that the stage I model fits well up to about 0.88 relative density but increasingly rises with respect to the data above this value. Similarly, the stage II model fits the data in its own density range (above 0.9) but does not fit the data outside its range. There is a discontinuity in the slope of the curves at the intersection of the stage I and stage II curves. This indicates that simple switching from stage I to stage II model is inadequate for densification prediction. Furthermore, discontinuities are also exhibited by the radial and hoop stress components. This is shown for the radial stress by the dotted curve in Fig. 4. The reason for the stress discontinuity is related to the fundamental differences between the two models of densification. The open-porosity assumption of the stage I model leads to an elastic behaviour of the compact where the radial stress is only a fraction of the axial compression. In contrast, the closed-pore assumption for stage II leads to an equilibrated fluid-like behaviour where the stress is close to hydrostatic, i.e., the radial and hoop stresses have similar magnitudes to the applied axial stress.

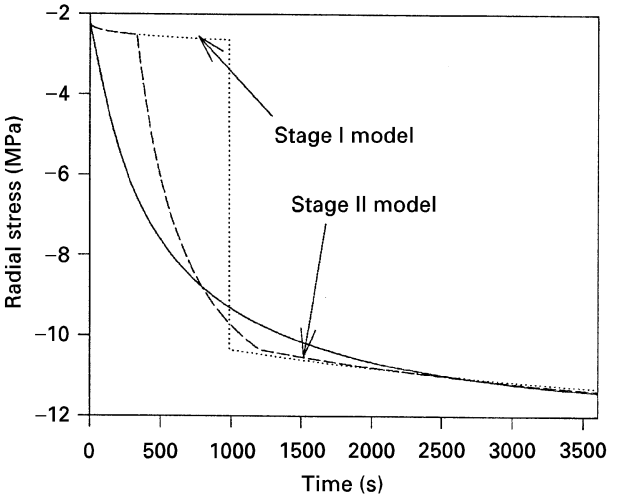

Figure 4 Comparison of radial stress histories obtained by blending of the stage I and stage II models (alumina powders hot pressed at 12 MPa and 1450 °C). (···), no blending; (– – –), linear blending; (—), cubic blending.

5. Model blending

To eliminate the discontinuity in the slope of the predicted densification curve, Song *et al.* [6] suggested blending the two models as follows:

$$\dot{E}_{ij} = w_1(D)(\dot{E}_{ij})_{\mathrm{I}} + w_2(D)(\dot{E}_{ij})_{\mathrm{II}} \qquad (20)$$

where $(\dot{E}_{ij})_{\mathrm{I}}$ and $(\dot{E}_{ij})_{\mathrm{II}}$ are the components of the creep strain rate tensors (Equations 1 and 6) and $w_1(D)$ and $w_2(D)$ are linear interpolation polynomials given as

$$w_1(D) = \frac{D_2 - D}{D_2 - D_1} \qquad (21)$$

$$w_2(D) = \frac{D - D_1}{D_2 - D_1} \qquad (22)$$

where D_1 and D_2 define the blending region. Song *et al.* [6] used $D_1 = 0.8$ and $D_2 = 0.9$ to give a blending region of 0.1.

This method of blending was applied for the prediction of densification of the alumina cylinders hot pressed in the experimental part of this study. Although the density prediction is reasonably smooth as shown in Fig. 5, there exists a discontinuity in the slopes of the radial and hoop stresses, as shown for the radial stress in Fig. 4 by the broken curve. Although this discontinuity is not as severe as that without blending, it is unlikely that in nature the development of stress would show sudden changes in slope. It is more likely that the stresses would change more gradually from an elastic state (stage I) to a hydrostatic state (stage II). To be able to predict such a gradual change it is proposed to blend the stage I and stage II models from the onset of densification ($D = D_0$) to the end at full density ($D = 1.0$). The physical argument for this is that the average porosity in the compact is

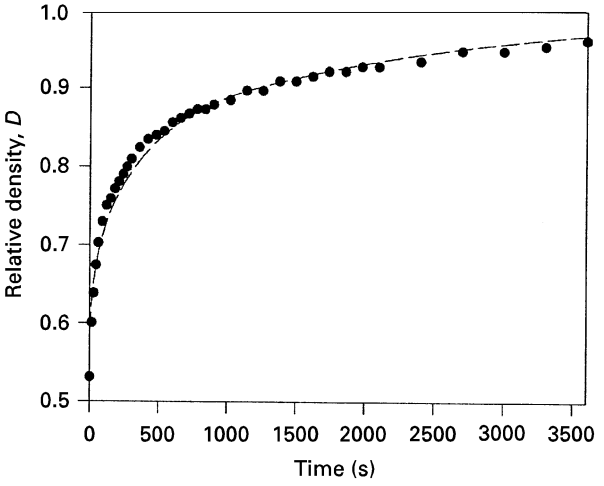

Figure 5 Predicted densification behaviour of alumina powders during hot pressing under 12 MPa at 1450 °C by linear blending (– – –) of the stage I and stage II models. (●), experiment.

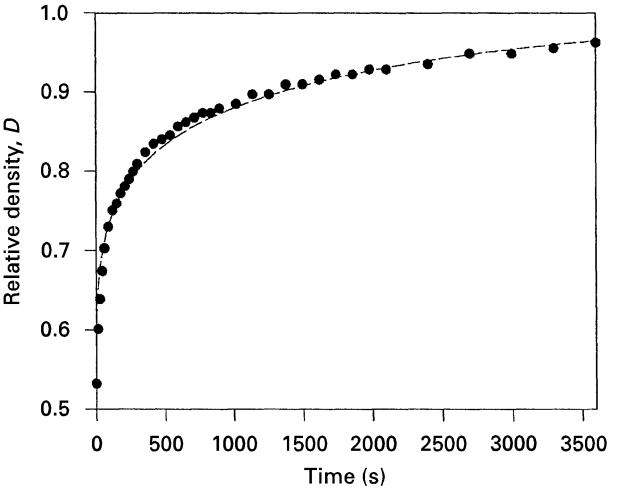

Figure 6 Predicted densification behaviour of alumina powders during hot pressing under 12 MPa at 1450 °C by the unified model (– – –). (●), experiment.

likely to shift gradually from completely open (stage I) to completely closed (stage II) with increase in density. Accordingly, blending was done using cubic interpolation polynomials in Equation 20, namely,

$$w_1(D) = 1 - 3s^2 + 2s^3 \quad (23)$$

$$w_2(D) = s^2(3 - 2s) \quad (24)$$

$$s = \frac{D - D_0}{D_2 - D_0} \quad (25)$$

where D_0 and D_2 are the relative densities at the start and the end respectively, of densification. This broad range blending of the stage I and stage II models will be referred to as the "unified" densification model.

The fit of the unified model to the densification data for the cylindrical alumina compact at an applied pressure of 12 MPa and a temperature of 1450 °C is shown in Fig. 6. As seen in the figure, the model fits the data well and does not have a discontinuity in the slope of the density curve. The corresponding radial stress history, shown in Fig. 4 by the solid curve, is without discontinuities both in magnitude and in slope. The transition is smooth from the initial elastic state of stress to the final hydrostatic state at the end of compaction. The unified model also predicted a smooth evolution of the hoop stress. It should be noted that during compaction there is no change in the axial stress component due to the uniaxial geometry.

In addition to the 12 MPa applied pressure case, the unified model was also fitted to data for applied pressures of 5 and 7 MPa at 1450 °C and 20 MPa at 1400 °C. The constants initially estimated from the 12 MPa, 1450 °C data were adjusted by trial and error to minimize the least-squares error between the unified model prediction and the data simultaneously for all the applied pressures at the two temperatures. The resulting best fit constants are shown in Table I.

The overall good fit of the unified model to the data for the applied pressures of 5, 7 and 12 MPa at 1450 °C are shown in Fig. 7. Using the constants shown in Table I, densification predictions were made

TABLE I Creep constants for the unified model

A_1^*	4.6×10^3 MPa^{-2} s^{-1}
A_2^*	1.52 MPa^{-2} s^{-1}
n_1	2
n_2	1
Q_1	300 kJ mol^{-1}
Q_2	171 kJ mol^{-1}

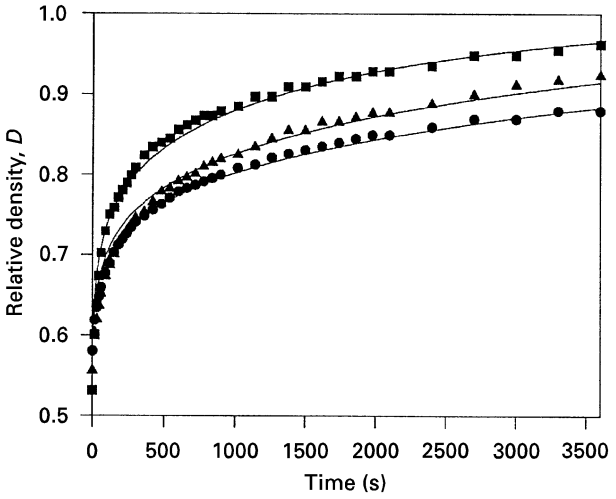

Figure 7 Comparison between predictions of unified model (—) with experimental data for different applied pressures ((●), 5 MPa; (▲), 7 MPa; (■), 12 MPa) at 1450 °C.

for applied pressures of 5 and 10 MPa at 1400 °C. It should be noted that the 5 and 10 MPa data at 1400 °C were not used to obtain the model constants. The good fit between the predictions and the data is shown in Fig. 8. Furthermore, the radial and hoop stresses for all pressures were found to be free of discontinuities.

6. Discussion

Uniaxial hot pressing is a densification process in which the state of stress varies from essentially elastic

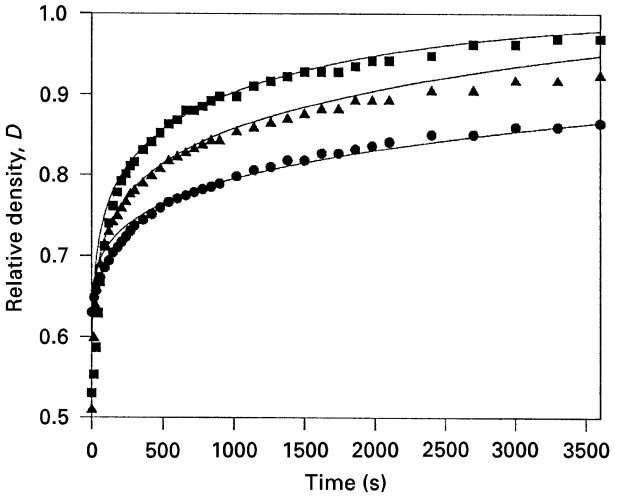

Figure 8 Comparison between predictions of unified model (—) with experimental data for different applied pressures ((●), 5 MPa; (▲), 10 MPa; (■), 20 MPa) at 1400 °C.

at the beginning to hydrostatic at the end of compaction. The radial and hoop stresses in uniaxial hot pressing are caused by constrained lateral expansion, and they depend on the powder compact's Poisson's ratio and elastic modulus. For the alumina powder considered in this research these lateral stresses initially amount to 20–25% of the applied axial stress. Another way of stating this is that the stress tensor of an uniaxially loaded elastic body has significant deviatoric stress components. It is expected that the lateral stresses will equilibrate with the axial stress because of creep-induced stress relaxation as densification progresses. The state of stress will eventually become hydrostatic and the stress tensor will lose its deviatoric component. The rate of stress relaxation depends on the rate of densification and the concurrent creep.

The densification models discussed in this paper predict stress evolution differently from each other. As can be seen in Fig. 4 by the dotted cure, the stage I model predicts a rather slow change in the radial stress from the initial elastic value towards the applied axial stress. Specifically, at the end of applicability of the stage I model ($D = 0.9$) the radial stress changed only a few per cent from its initial value. Similarly, the stage II model also predicts a relatively slow change in the lateral stresses with time (Fig. 4), but according to the prediction the magnitude of the lateral stresses is close to the applied axial stress throughout the stage II applicability range ($D = 0.9$–1.0). This result in a large difference between the radial stress predictions by the stage I and stage II models, and hence the apparent discontinuity at $D = 0.9$.

It is believed that the problem lies not with the models but with the assumption that the powder compact's porosity is either entirely open or entirely closed, as would be required by separately using the models in their respective relative density ranges. A more likely situation is that both open and closed pores exist simultaneously in the compact and only their relative number changes with respect to each other. The compact may start out with 100% open porosity but, as the density increases, the smaller pores would begin to close up and the larger pores remain open for a longer period. The successive closing of pores would lead to a gradual shift from a completely open to a completely closed porosity. This is the situation that is represented by the unified model. In this model the mechanism of densification as postulated by Kuhn and McMeeking [1] and Sofronis and McMeeking [2] is unaltered; only the assumption regarding the character of porosity is changed.

There are no experimental data available at this time on the relative ratio of open to closed pores as a function of density during hot pressing. Therefore, the proposed blending model, i.e., the cubic interpolation between stage I and stage II, is only a first attempt to represent properly the change in porosity with density. As detailed porosity data become available, the method of blending can be refined.

Direct observation of the state of stress during hot pressing is not possible. Therefore, comparison between the predicted and actual stresses can only be made in terms of the residual stresses that remain in the compact after densification. Validation of the proposed unified model must be done with experiments that lead to significant deviatoric stresses, and hence significant level of residual stresses, at the end of compaction. A likely candidate for such experiments is hot pressing compacts with initial gradients in their properties, such as green density or composition.

The question may arise why should one worry about the prediction of stress if the density can already be predicted correctly with the existing densification models. In response, it should be pointed out that previous models predict density correctly only in cases when no significant deviatoric stresses develop during densification, such as HIP. This is because these are the only cases where the prediction does not result in stress discontinuity. If the stress prediction is wrong it is reasonable to assume that the density prediction is also in error since densification is driven by stress. Therefore, the previous models cannot be used to predict densification and stress evolution in cases such as HIP or hot pressing with green density or temperature gradients, die wall friction, and other heterogeneities in the compact. For these cases the unified model is believed to be the appropriate model to use.

7. Conclusions

Discontinuity in the densification rate and stress state was discovered when predicting hot pressing of cylindrical compacts with existing power-law creep densification models. Blending of the existing models was used to develop a new densification model which was able to predict densification and stress evolution without a discontinuity. The material constants used in this new unified model were obtained by fitting the model to experimental data, for homogeneous alumina powders hot pressed at 1400 and 1450 °C with different pressures. The unified model fit the data well and exhibited a smooth increase in density and a smooth transition of the radial and hoop stresses from a nearly elastic to a hydrostatic state. Future research will involve prediction of densification

behaviour and the development of residual stresses during hot pressing of compacts with property gradients such as initial green density and composition.

References

1. L. T. KUHN and R. M. MCMEEKING, *Int. J. Mech. Sci.* **34** (1992) 563.
2. P. SOFRONIS and R. M. MCMEEKING, *J. Appl. Mech.* **59** (1992) S88.
3. M. F. ASHBY, in "HIP 6.0—background reading" (Engineering Department, University of Cambridge, 1990).
4. M. ABOUAF, J. L. CHENOT, G. RAISSON and P. BAUDUIN, *Int. J. Numer. Method Engng* **25** (1988) 191.
5. Y. M. LIU, H. N. G. WADLEY and J. M. DUVA, *Acta Metall.* **42** (1994) 2247.
6. M. C. SONG, H. G. KIM and K. T. KIM, *Int. J. Mech. Sci.* **38** (1996) 1197.
7. "ABAQUS/standard user's manual" (Hibbitt Karlsson and Sorensen, Pawtucket, RI, 1995.
8. B. BUDIANSKY, *J. Compos. Mater.* **4** (1970) 286.
9. M. WESTORT, Master's Thesis, Department of Mechanical and Industrial Engineering, University of Massachusetts, Amherst, MA (1996).

Received 27 March
and accepted 29 May 1997